

## "Seismic Ground Motion Incoherency Effects on Soil-Structure Interaction Response of NPP Building Structures"

Dan M. Ghiocel \* and Farhang Ostadan \*\*

\*) Ghiocel Predictive Technologies, 6 South Main St, Pittsford NY 14534, USA

\*\*\*) Bechtel Corporation, 50 Beale Street, PO Box 193965, San Francisco, CA 94119, USA

### ABSTRACT

The paper illustrates the effects of ground motion incoherency on seismic SSI responses of a typical axisymmetric nuclear reactor building and two industrial buildings with significant mass eccentricities. To incorporate the motion incoherency effects on SSI response we used both stochastic and deterministic approaches (Ghiocel, 2005, 2006, Ostadan, 2005, 2006, Ostadan and Ghiocel, 2007). In this study two the plane-wave coherency models are used: i) the Luco-Wong coherency model (Luco and Wong, 1986) and, ii) the Abrahamson incoherency model (Abrahamson, 2005). The motion incoherency approaches are comparatively applied for coherent and incoherent seismic input motions to illustrate the effects of motion incoherency on SSI response. The SSI coupling responses of structures are primarily examined to illustrate the additional rocking and torsional motion effects due to the motion incoherency. The SSI results in terms of transfer functions, acceleration response spectra and structural forces are obtained to study the motion incoherency effects. The study shows that incoherency effects are significant in the high-frequency ranges and much less significant for the low frequency responses.

### SEISMIC MOTION INCOHERENCY MODELING

Assuming that the seismic wave field,  $U$ , can be modeled by a plane wave motion, the cross-spectral density of motion stochastic field for two points  $i$  and  $k$ , can be expressed by

$$S_{U_i, U_k}(\omega) = [S_{U_i, U_i}(\omega)S_{U_k, U_k}(\omega)]^{1/2} \text{Coh}_{U_i, U_k}(\omega) \quad (1)$$

where is the cross-spectral density function for point motions  $U_i$  and  $U_k$ , and ,  $j = i, k$  is the auto-spectral density for location point  $j$ . Inversely, from equation (1), the coherence between the two arbitrary motions can be derived as a complex function of frequency:

$$\text{Coh}_{U_j, U_k}(\omega) = \frac{S_{U_j, U_k}(\omega)}{[S_{U_j, U_j}(\omega)S_{U_k, U_k}(\omega)]^{1/2}} \quad (2)$$

The coherence is a measure of the similarity of the two point motions, including both the amplitude spatial variation and the wave passage effects.

There are several ways of describing motion incoherency using either i) the lagged coherency function, ii) the plane-wave coherency function, or iii) the unlagged coherency. Abrahamson describes these three types of coherency as follows (Abrahamson, 2005):

1) The lagged coherency is the most commonly cited as coherency measure or coherence spectrum. It is the coherency measured after aligning the time series using the time lag that leads to the largest modulus of the cross spectrum. There is no requirement that the time lags are consistent between frequencies. In general, the lagged coherency does not go to zero at large separations and high frequencies.

2) The plane-wave coherency differs from the lagged coherency in that it uses a single time lag for all frequencies. That is, it measures the coherency relative to a single wave speed for each earthquake. As a result, the plane-wave coherency is smaller than the unlagged coherency. The plane-wave coherency is found by taking the real part of the smoothed cross-spectrum after aligning the ground motions on the best plane-wave speed. The plane-wave coherency function approaches zero at high frequencies and large separations.

3) The unlagged coherency measures the coherency assuming no time lag between locations. It is the real part of the smoothed cross-spectrum. The unlagged coherency will be smaller than the plane-wave coherency. The coherent part of the wave passage effect can lead to negative values of the unlagged coherency.

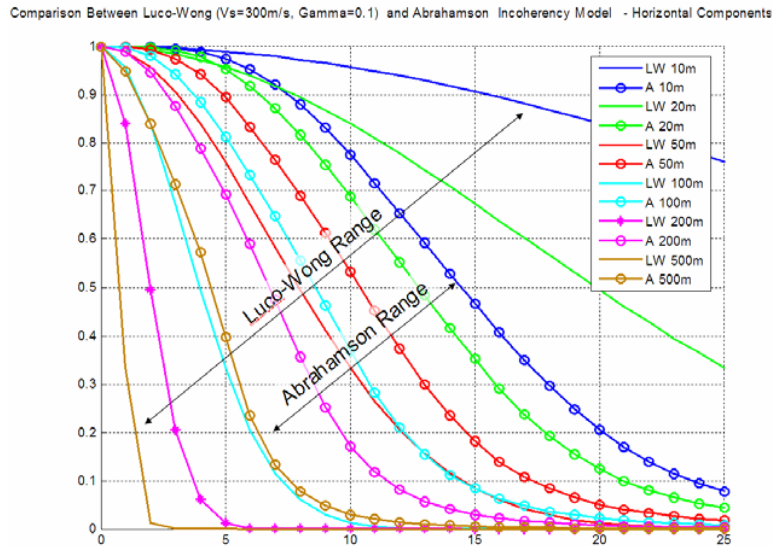


Figure 1. Comparative Coherency Function Variations for Different Distances; Luco-Wong Model (1986) vs. Abrahamson Model (2005)

In this paper we idealized seismic motion incoherency using the Luco-Wong and Abrahamson plane-wave coherency models described elsewhere (Luco and Wong, 1986, Abrahamson, 2005). As shown in Figure 1, the two coherency functions differ significantly for large and short distances. The Luco-Wong coherency model is an analytical, physics-based model based on the physics of wave propagation in random media. The Abrahamson model is an empirical-based model based on many recorded datasets from various earthquake motions observed in dense arrays. Figure 1 indicates that Luco-Wong model has a higher sensitivity with respect to the distance variation than Abrahamson model.

To incorporate the random motion incoherency effects on SSI response two types of approaches are used: i) Stochastic Approach (SA) based on using Monte Carlo for simulating a set of random realizations of spatial motion variation (Ghiocel, 2002, 2005, 2006), and ii) Deterministic Approach (DA) based on approximating the stochastic spatial motion variation by a single realization or SSI analysis run (Ghiocel, 2004, 2006, Ostadan, 2005, 2006).

SA uses a SSI initiation run to perform the spectral factorization of the foundation coherency matrix and to compute the structural transfer functions for all SSI model degrees of freedom. The other random realizations are then computed fast by using an advantageous restart option that uses the saved information coherency kernel factorization and transfer function computed by the initiation SSI run.

DA is also based on the spectral factorization of coherency kernel, but assumes, instead of random combination of different wavelength components, deterministic combinations of different wavelength components. Two DA alternatives are implemented based on 1) Linear Superposition of different wavelength components of the free-field incoherent motion (DALs) and 2) quadratic superposition based SRSS combination of SSI complex frequency responses computed for different wavelength components (DAQS).

## CASE STUDIES

### Reactor Building Structure

A Reactor Building with axisymmetric containment shell and internal structures was considered using Luco-Wong model. The coherence parameter was assumed to be 0.10. The soil was modeled as a viscous elastic half-space with a  $V_s = 1000$  fps. No wave passage was considered. The DALs approach was used to compute motion incoherency effects. The computed

coherent and incoherent acceleration amplitude transfer functions and in-structure spectra are compared in Figures 2 and 3. The incoherent SSI analysis results indicate a significant reduction of in-structure floor spectra in high-frequency range, although the incoherency effects for a 0.10 coherence parameter are reduced. These results indicate that there is a significant reduction of the in-structure response spectra due to motion incoherency effects. Thus, the inclusion of motion incoherency as a design basis procedure brings a significant cost saving by reducing the seismic demand for many nuclear equipment systems.

**Industrial Building with Large Mass Eccentricity**

This case study illustrates the effects of motion incoherency on SSI response of a non-symmetric building with a large mass eccentricity. The industrial building with a relatively poor seismic design with a “L-shaped” concrete-steel building. The soil layering with a viscous half-space with a  $V_s = 1000$  fps. The foundation consists of isolated foundations under the walls and columns. Motion incoherency effects were computed using Luco-Wong model for a coherence parameter of 0.4. No wave passage was considered. The DALS approach was used. Figures 4 and 5 show the computed amplitude transfer functions of acceleration response at the building roof level for two diagonal corners. The two roof corners are the roof corner (node 31) above the "stiff" concrete part of the building and the roof corner (node 45) above the "flexible" steel part of the building. The computed transfer functions indicate a large response amplification of motion at the "flexible" corner. The seismic coupling responses in a perpendicular direction to the input motion direction, not shown herein, were significant, indicating a significant torsional SSI response. The spectral peaks of transfer functions at the two roof corners, "stiff" corner (node 31) and "flexible" corner (node 45), were 30% and 60%, respectively, higher for the incoherent motion than for the coherent motion. For the corner column situated under the "flexible" roof part, the maximum bending moment increased by 50% due to motion incoherency effects.

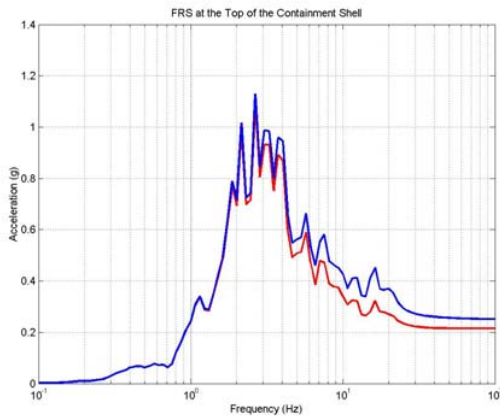


Figure 2. ARS at Top of Containment Shell

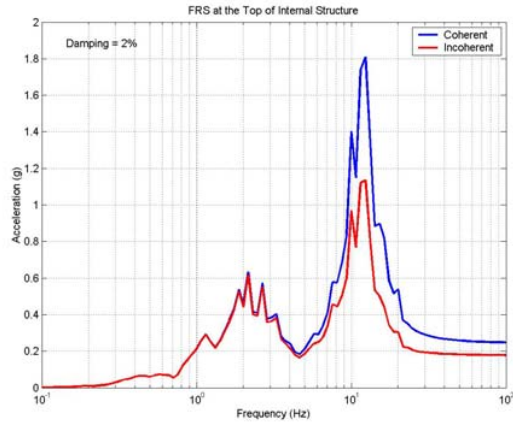


Figure 3. ARS at Top of Internal Structure

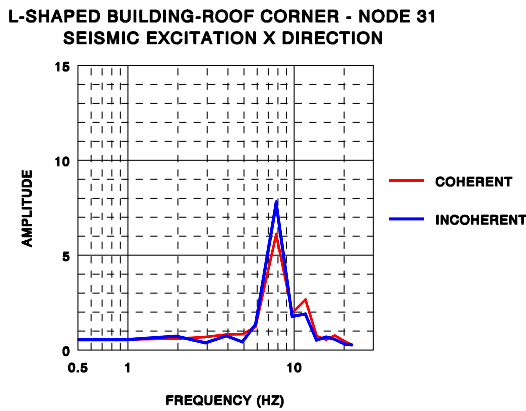


Figure 4. ATF at the Roof Level (concrete)

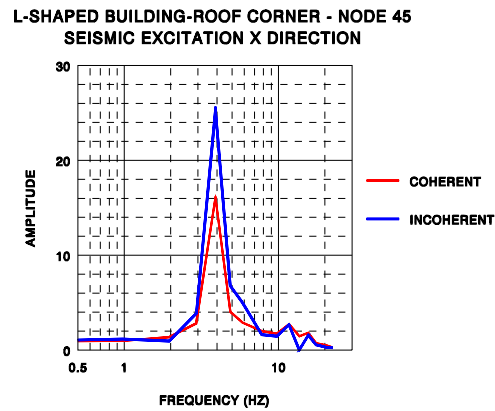


Figure 5. ATF at the Roof Level (steel)

**Multiple Structures on Common Basemat**

This example illustrates the effects of motion incoherency for an industrial facility founded on a rock site. The seismic input motion is very rich in high-frequency components.

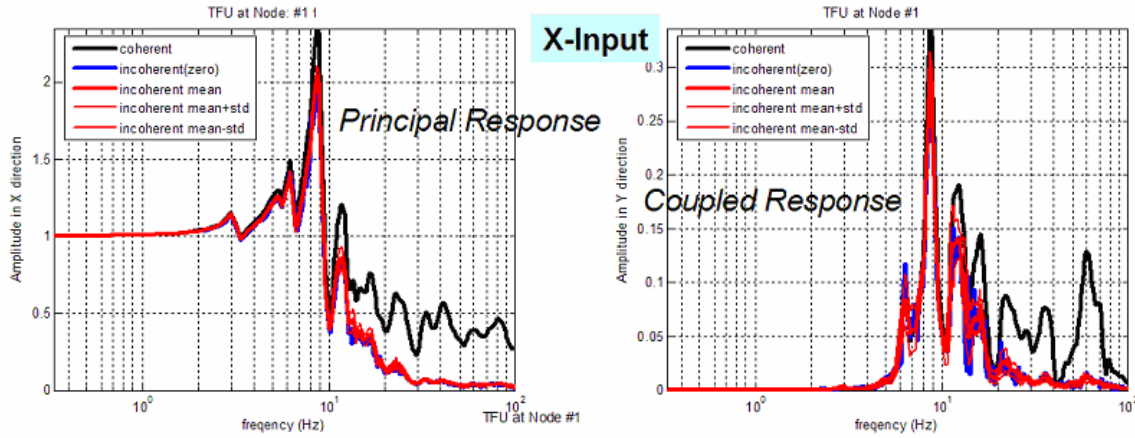


Figure 6 Coherent vs. Incoherent Amplitude Transfer Functions at Basemat Center (Node 1) for X-shaking

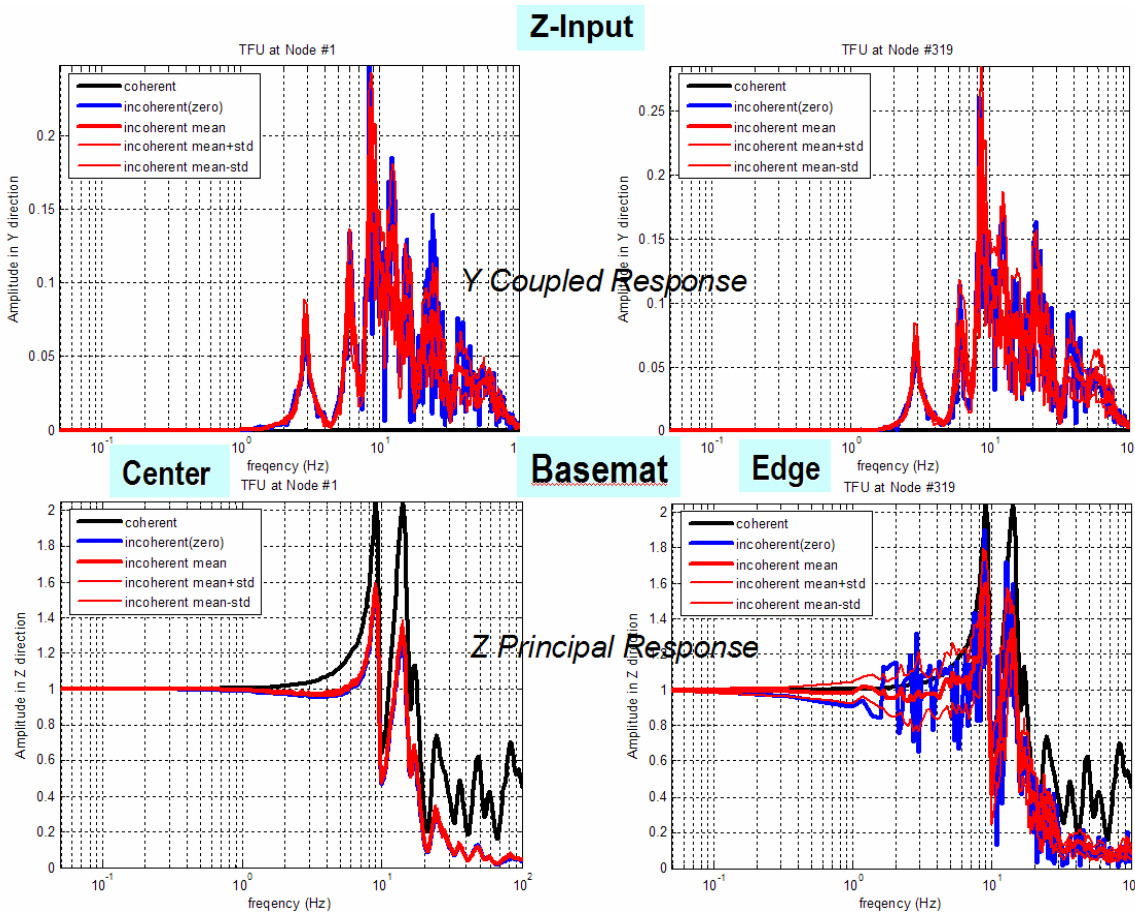


Figure 7 Coherent vs. Incoherent Amplitude Transfer Functions at Basemat Center (Node 1) and Edge (Node 319) for Z-shaking

The 2005 Abrahamson model was applied. No wave passage was considered. Both the SA and DA approaches were applied. The results of stochastic approach were based on statistical averaging of 20 random realization of the random spatial variation of input motion.

Figures 6 and 7 show the computed coherent and incoherent amplitude transfer functions (ATF) at the basemat level for X- and Z- direction shakings. The effect of motion incoherency of reducing the ATF values in high-frequency range is obvious.

Figures 8 and 9 show the computed coherent vs.. incoherent acceleration response spectra at foundation level (node 1 centric) and at in-structure level (node 29-centric and node 229-eccentric). Figure 8 shows that for horizontal X-input, the coherent responses are higher for centric locations in the direction of the excitation, and also for eccentric in-structure locations sensitive to basemat rocking motion.

Figure 9 shows that for vertical Z-input, the coherent responses are higher for centric locations in the direction of the excitation (node 29Z). The ARS plots indicate that the stochastic effects coming from motion incoherency do not depend significantly on the random phases of different input motion wavelength components. The statistical ARS curves (three red lines) computed using SA indicate a reduced standard deviation values (coefficients of variation in the 10%-20% range). The ARS computed using DA, specifically DALs (denoted “incoherent LSP” in the legend) and DAQS (denoted “incoherent SRSS” in the legend), show the approximate superposition rules of different input wavelength components (in DALs) or output wavelength components (in DAQS) are close to the mean ARS computed by statistical averaging using SA.

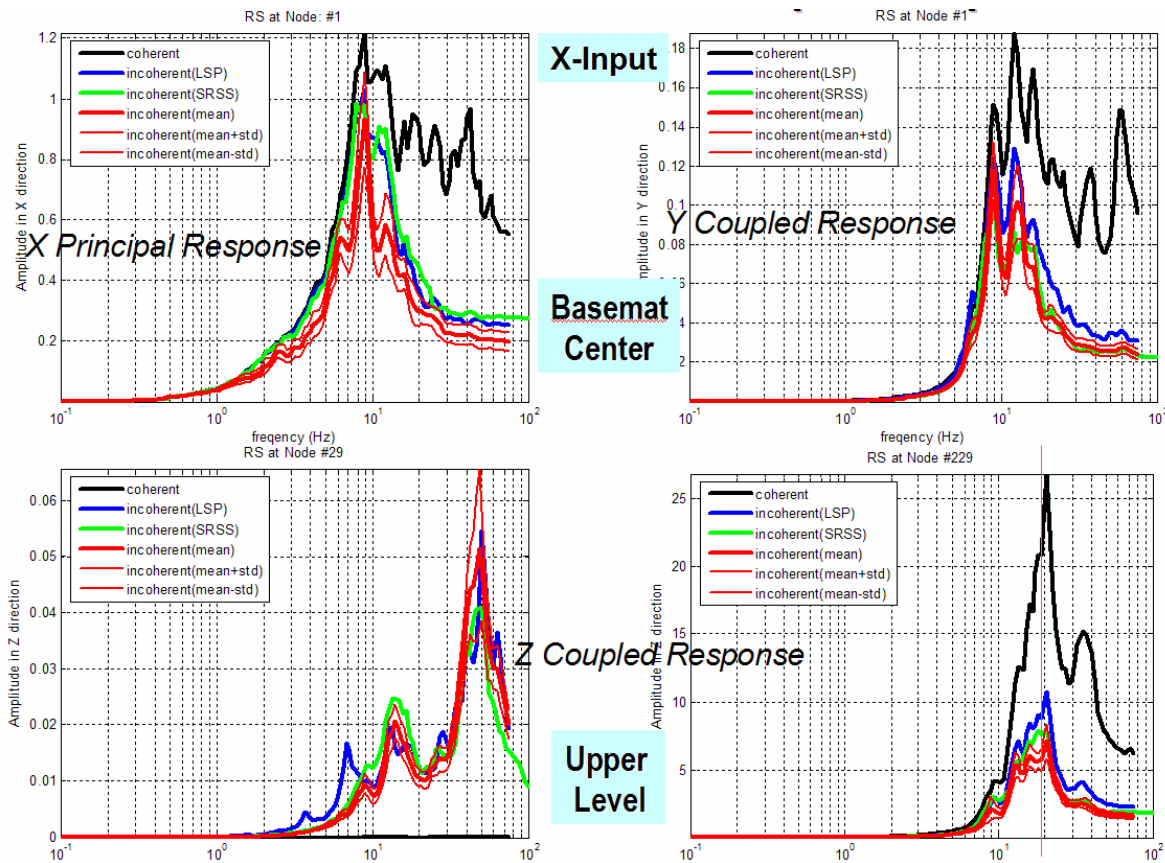


Figure 8 Coherent vs. Incoherent Computed ARS at Basemat and In-Structure for X-Input Direction; SA (red lines for statistical curves), DALs (blue line), DAQS (green line)

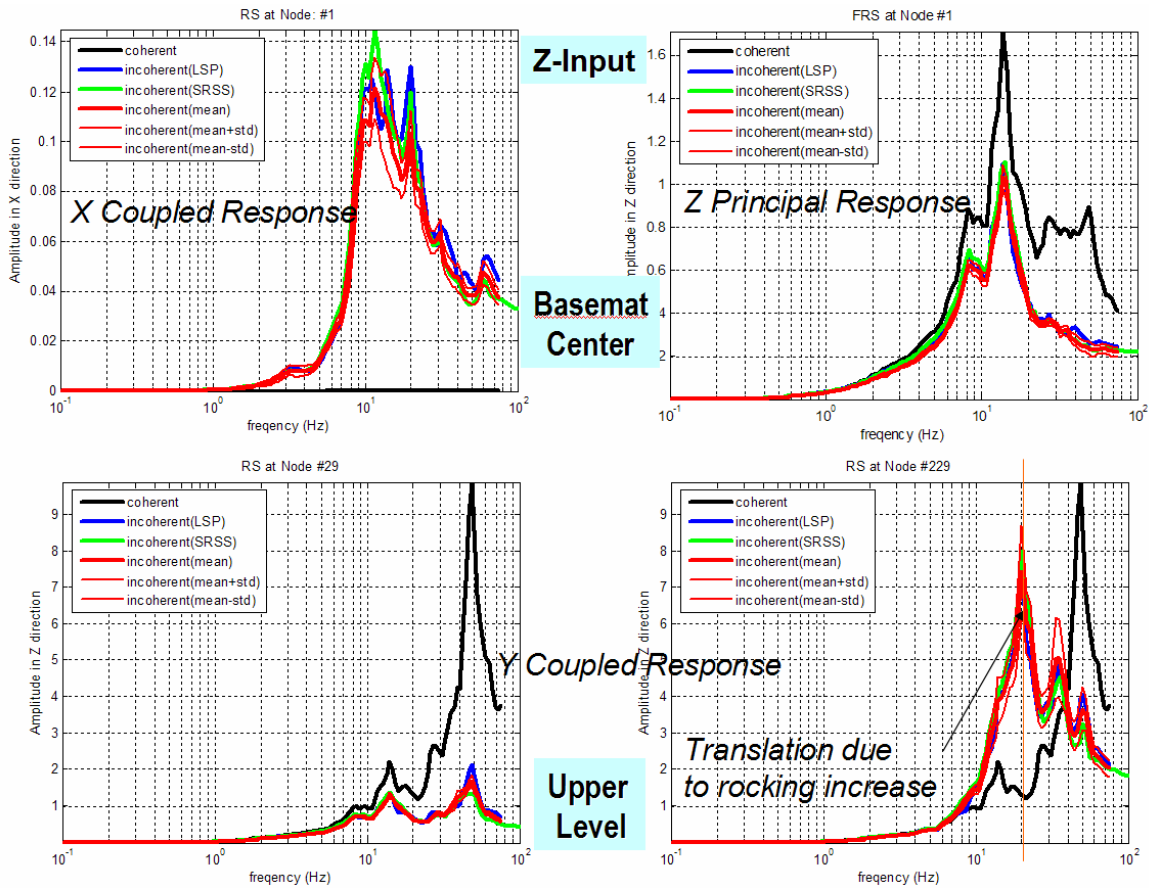


Figure 9 Coherent vs. Incoherent Computed ARS at Basemat and In-Structure for Z-Input Direction; SA (red lines for statistical curves), DALs (blue line), DAQS (green line)

It should be noted that, in general, the motion incoherency effects are favorable to SSI response by reducing the computed in-structure ARS in the high-frequency range. However, exceptions can be also noted. For the Z-shaking, the effect of incoherency-induced rocking motions is to amplify the vertical translation of the eccentric node 229 for the 20Hz SSI translational mode as illustrated in Figure 9, lower-right side plot.

**CONCLUSIONS**

The illustrated SSI examples have shown that incoherency effects are significant in the high-frequency ranges. As a result of this, the incoherency effects affect less significantly the low-frequency, overall seismic structural responses, namely the structural shear and moments, but more significantly the high-frequency vibration modes and in-structure response spectra. The qualitative effects of motion incoherency effects are: i) for horizontal components a reduction in excitation translation along the input direction concomitantly with an increase in torsional excitation and a slight reduction in foundation rocking excitation and ii) for vertical component a reduction in excitation translation in vertical direction concomitantly with an increase of rocking excitation.

Due to the complex and significant effects of motion incoherency on SSI response, it is important to consider motion incoherency effects on seismic design of hazardous facilities, federal buildings and life lines. The future coming revised engineering design standards will include the necessary practical guidelines on how to consider the motion incoherency effects for the new designs of advanced nuclear reactor facilities.

## REFERENCES

1. Abrahamson, N., (1993) "Spatial Variation of Multiple Support Inputs", the 1st US Seminar on Seismic Evaluation and Retrofit of Steel Bridges, University of California at Berkeley, San Francisco, October.
2. Abrahamson, N. (2005) "Spatial Coherency Models for Soil-Structure Interaction", Draft EPRI Report, July.
3. Ghiocel, D.M. R. (2002) "Stochastic Finite-Element Analysis of Seismic Soil-Structure Interaction", ASCE, Journal of Engineering Mechanics, Vol. 128, No. 1, January.
4. Ghiocel, D.M. and Wang, L. (2004) "Seismic Motion Incoherency Effects on Structures", Proceedings 3rd UJNR Workshop on Soil-Structure Interaction, March 29-30, 2004, Menlo Park, California, March 30-31.
5. Ghiocel, D.M. (2005) "Stochastic Simulation Methods in Engineering Predictions", Chapter 20 of "Engineering Design Reliability Handbook", Editors: Nikolaidis, Ghiocel and Singhal, CRC Press, Taylor & Francis, January.
6. Ghiocel, D.M. (2006) "ACS SASSI Version 2.2 – An Advanced Computational Software for System Analysis for Soil-Structure Interaction; User Manuals", Technical Report, Rochester, New York.
7. Luco, J. E. and Wong, H.L (1986) "Response of Rigid Foundation to Spatially Random Ground Motion", Journal of Earthquake Engineering & Structural Dynamics, Vol.14, pp. 891-908.
8. Mita, A. and Luco, J.E., (1986) "Response of Structures to A Spatially Random Ground Motion", the 3rd U.S. National Conference on Earthquake Engineering, p. 907-918, Charleston, North Carolina.
9. Ostadan, F. and Ghiocel, D.M. (2007) "SASSI2007 - A System for Analysis of Soil-Structure Interaction; User Manuals", Joint Technical Report with University of California, Berkeley, San Francisco, California (in progress).
10. Ostadan, F. (2006) "SASSI2000 - A System for Analysis of Soil-Structure Interaction, User Manuals, Revision 2", Technical Report, San Francisco, California.
11. Ostadan, F, Deng, N, Kennedy, R (2005) "Soil-Structure Interaction Analysis Including Ground Motion Incoherency Effects", 18th International Conference on Structural Mechanics in Reactor Technology (SMiRT 18) Beijing, China, August 7-12, 2005, SMiRT18-K04-7